ANTIOXIDANTS & REDOX SIGNALING
Volume 26, Number 8, 2017

DOI: 10.1089/ars.2016.6715

FORUM ORIGINAL RESEARCH COMMUNICATION

Blockade of Glutamine Synthetase Enhances Inflammatory Response in Microglial Cells

Erika M. Palmieri,[1,*] Alessio Menga,[2,*] Aurore Lebrun,[3,4] Douglas C. Hooper,[3,4] D. Allan Butterfield,[5,6] Massimiliano Mazzone,[7,8] and Alessandra Castegna[1,2]

Abstract

Aims: Microglial cells are brain-resident macrophages engaged in surveillance and maintained in a constant state of relative inactivity. However, their involvement in autoimmune diseases indicates that in pathological conditions microglia gain an inflammatory phenotype. The mechanisms underlying this change in the microglial phenotype are still unclear. Since metabolism is an important modulator of immune cell function, we focused our attention on glutamine synthetase (GS), a modulator of the response to lipopolysaccharide (LPS) activation in other cell types, which is expressed by microglia.

Results: GS inhibition enhances release of inflammatory mediators of LPS-activated microglia *in vitro*, leading to perturbation of the redox balance and decreased viability of cocultured neurons. GS inhibition also decreases insulin-mediated glucose uptake in microglia. *In vivo*, microglia-specific GS ablation enhances expression of inflammatory markers upon LPS treatment. In the spinal cords from experimental autoimmune encephalomyelitis (EAE), GS expression levels and glutamine/glutamate ratios are reduced.

Innovation: Recently, metabolism has been highlighted as mediator of immune cell function through the discovery of mechanisms that (behind these metabolic changes) modulate the inflammatory response. The present study shows for the first time a metabolic mechanism mediating microglial response to a proinflammatory stimulus, pointing to GS activity as a master modulator of immune cell function and thus unraveling a potential therapeutic target.

Conclusions: Our study highlights a new role of GS in modulating immune response in microglia, providing insights into the pathogenic mechanisms associated with inflammation and new strategies of therapeutic intervention. *Antioxid. Redox Signal.* 26, 351–363.

Keywords: glutamine synthetase, glutamine, microglia, neuroinflammation, insulin resistance

Introduction

MICROGLIA ARE BRAIN-RESIDENT macrophages involved in the maintenance of central nervous system (CNS) homeostasis by continually surveying the extracellular environment (10). Once microglia encounter a harmful or foreign entity, they enter an activated state, regulating CNS innate immunity and initiating appropriate responses. These events, often leading to neuroinflammation, have the sole purpose to protect the CNS; however, uncontrolled or prolonged neuroinflammation is potentially harmful and can result in cellular damage. This is particularly relevant to neurodegenerative diseases, to which microglial activation and neuroinflammation have been associated (23, 59). The

[1]Department of Biosciences, Biotechnologies and Biopharmaceutics, University of Bari, Bari, Italy.
[2]National Cancer Research Center, Istituto Tumori 'Giovanni Paolo II,' Bari, Italy.
Departments of [3]Cancer Biology and [4]Neurological Surgery, Thomas Jefferson University, Philadelphia, Pennsylvania.
[5]Department of Chemistry, [6]Sanders-Brown Center on Aging, University of Kentucky, Lexington, Kentucky.
[7]Laboratory of Tumor Inflammation and Angiogenesis, Department of Oncology, University of Leuven, Leuven, Belgium.
[8]Laboratory of Tumor Inflammation and Angiogenesis, Vesalius Research Center, VIB, Leuven, Belgium.
*These authors contributed equally to this work.

Innovation

Recently, metabolism has been highlighted as an important mediator of immune cell function through the discovery of mechanisms that (behind these metabolic changes) strongly impact on immune function potentially modulating pathological events associated with inflammation. The present study shows for the first time a metabolic mechanism mediating microglial response to a proinflammatory stimulus, pointing to glutamine synthetase activity as a master modulator of immune cell function. Unraveling this mechanism is fundamental for both the understanding of the mechanisms, by which oxidative stress translates into inflammatory signals, and for setting up new diagnostic tools and strategies of therapeutic intervention.

discovery and the increasing interest in their function make microglia an attractive therapeutic target, particularly with respect to glutamate excitotoxicity. Indeed, the removal of glutamate by the concerted activity of the glutamate transporter (GLT-1), and glutamine synthetase (GS), which converts glutamate into the nontoxic glutamine (14, 19), is commonly accepted as a mechanism relevant to astrocytes (37, 47). However, GS and GLT-1 expression has been recently reported in microglia (12). Consequently, an astrocyte-like glutamate scavenging and neutralization process (through conversion to glutamine), which has been recently speculated to occur in microglia (48), may be mediated by microglia responding to inflammatory stimuli.

GS activity is evidently an element connecting glutamate metabolism to inflammation. Indeed, we have shown that GS expression desensitizes mature adipocytes to proinflammatory stimuli through the elevation of intracellular glutamine levels (50). This highlights a novel mechanism by which glutamine acts as signal molecule, leading to suppression of certain aspects of inflammation. A similar regulatory role of GS and glutamine has been noted in B cells, in which GS inhibits the mTOR pathway by raising intracellular glutamine (68). This novel function of GS in modulating the immune response through metabolism could be important in brain due to its expression in microglial cells. Important in this regard is the fact that brain GS, at variance with the liver and muscle isoform, is not feedback inhibited by glutamine (20). Furthermore, a strong body of evidence demonstrates that GS is highly sensitive to oxidants and therefore a fundamental redox target. Brain GS is a recognized target of oxidative stress in neurodegenerative disorders (8, 9) and in models of immune diseases through redox proteomic studies, and oxidative damage has been associated with reduced protein function (9).

Based on these data, we sought to investigate the role of GS expression and activity in lipopolysaccharide (LPS)-activated N9 and primary murine microglia to unravel the significance of its function with respect to microglial response to proinflammatory stimuli. Our results demonstrate that GS inhibition potentiates the microglial response to proinflammatory stimuli, leading to neuronal toxicity. In addition, the increased microglial inflammatory response is related to a reduced insulin-mediated glucose uptake. These data are translated *in vivo*, in which the response to LPSs of the microglial-specific GS conditional knockout (GScKO) mouse is strongly enhanced compared with the WT animal. GS function is also impaired in the spinal cord of mice with experimental allergic encephalomyelitis (EAE), in which microglia cells are known to play a role. These results unravel a novel mechanism by which the inflammatory response is endogenously controlled by GS expression and activity in microglia. The present findings also highlight a potential mechanism that through GS inhibition might lead to brain insulin resistance.

Results

GS is expressed in N9 activated with LPSs

To assess whether LPS can induce GS in N9 microglia in a time course manner, cells were incubated with LPSs (100 ng/mL) for 12, 24, 48, and 72 h. LPSs significantly increased GS activity strongly at 24 h after LPS treatment, then the enzyme activity decreased to reach control levels at 72 h (Fig. 1A). At variance with GS activity, the highest GS protein levels were reached only at 48 h after LPS treatment (Fig. 1B). These data demonstrate that microglial GS activity and expression are increased following LPS treatment. However, GS activity responds earlier after induction of a proinflammatory stimulus and this is not synchronized with GS protein expression, which increases at a later time point as similarly described by others (48).

GS inhibition enhances the inflammatory response of N9 microglia

To establish the role of GS in activated microglia, we treated N9 cells with LPS for 24 h in the presence of the GS inhibitor, methionine sulfoximine (MSO), which does not influence cell viability at a concentration up to 5 mM (Fig. 1C). In line with induction of GS activity, LPSs significantly increased the intracellular glutamine-to-glutamate ratio by 114%, which was promptly reversed by treatment with MSO (Fig. 1D). We also measured the levels of glutamate and glutamine in the microglial media following an LPS or LPS/MSO stimulation for 24 h. As expected, in media harvested from LPS-treated microglia, the glutamate/glutamine ratios were 63% higher (Fig. 1E) compared with resting microglia. However, MSO treatment strongly reverted this effect as the ratio decreased by 51% and by 70% compared with control and LPS-treated cells, respectively. These data demonstrate that extracellular glutamate levels are affected by GS inhibition. We then wanted to ascertain whether increased medium glutamate was also accompanied by an increase in the N-methyl-D-aspartate (NMDA) agonist, quinolinic acid, which is known to be released by activated microglia (23, 36). Although in N9 cell line the levels of quinolinic acid were not significantly higher in LPS-stimulated cells compared with control cells, MSO treatment increased by 100% the level of quinolinic acid measured in the media of LPS-treated cells, indicating that GS inhibition in microglia might induce NMDA receptor activation in neurons by releasing quinolinic acid (Fig. 1F).

GS inhibition enhances the inflammatory response of N9 and primary microglia

We then evaluated extracellular release of different mediators of the inflammatory response such as PGE2, IL-6, nitric oxide (NO), and reactive oxygen species (ROS) in N9

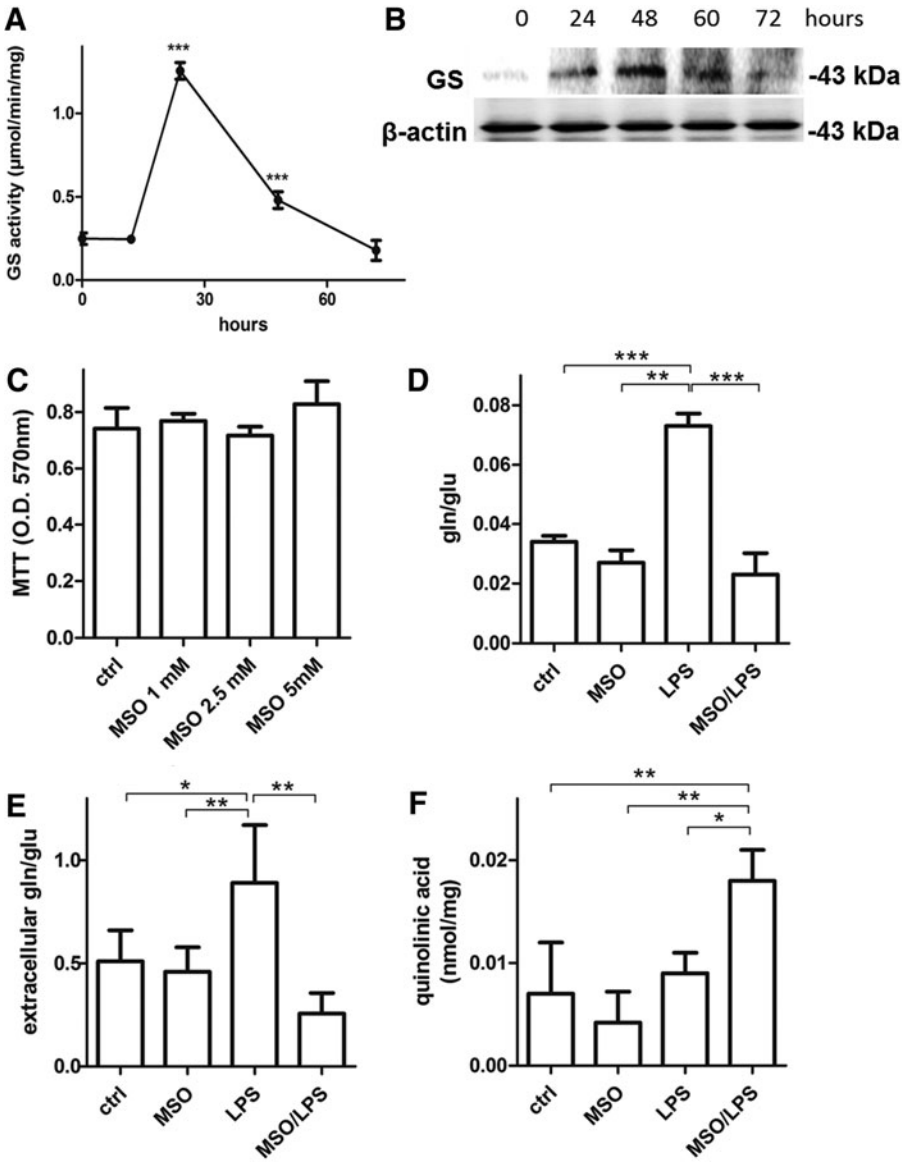

FIG. 1. Evidence of GS activity in LPS-activated microglia. **(A)** GS activity was measured in LPS-activated microglia at 16, 24, 48, and 72 h from the applied proinflammatory stimulus. The results are presented as mean ± S.D. of four independent experiments. Activity levels significantly higher than those measured at time zero are denoted as follows: ***$p < 0.0001$. **(B)** GS and β-actin protein level was assessed by Western blotting analysis on LPS-activated microglia harvested at the same time points. **(C)** Viability was tested on resting microglia incubated up to 48 h with increasing MSO concentrations, ranging from 1 to 5 mM. The results are presented as mean ± S.D. of five independent experiments. **(D)** LPS challenge was carried out for 24 h on microglial cells pretreated or not with 1 mM MSO. Intracellular **(D)** and extracellular **(E)** glutamine and glutamate levels and extracellular quinolinic acid **(F)** were measured by LC-MS/MS analysis. The results are presented as mean ± S.D. of four independent experiments. Glutamine/glutamate ratios and quinolinic acid levels are significantly higher than those measured in untreated control microglia cells and are denoted as follows: *$p < 0.05$, **$p < 0.001$, and ***$p < 0.0001$. GS, glutamine synthetase; LPS, lipopolysaccharide; MSO, methionine sulfoximine.

cells under LPS stimulus. LPS treatment produced a significant increase of IL-6 (Fig. 2B) and NO (Fig. 2C). GS inhibition substantially enhanced the proinflammatory effects of LPS-activated cells evaluated by a 58% increase of PGE2 (Fig. 2A), 106% increase of IL-6 (Fig. 2B), and 65% and 22% increase of NO (Fig. 2C) and ROS (Fig. 2D), respectively, compared with those observed after treatment with LPS alone. A similar effect was measured in primary murine microglia, in which LPS treatment in the presence of MSO induced 189%, 206%, and 104% increase in the release of PGE2 (Fig. 2E), IL-6 (Fig. 2F), and IL-12 (Fig. 2G), respectively, compared with LPSs alone. In all cases, treatment with MSO alone (no LPSs) did not produce any change in the evaluated parameters. These data together indicate that the inflammatory capacity of both N9 and primary microglia under LPS stimulus is greatly enhanced by GS inhibition.

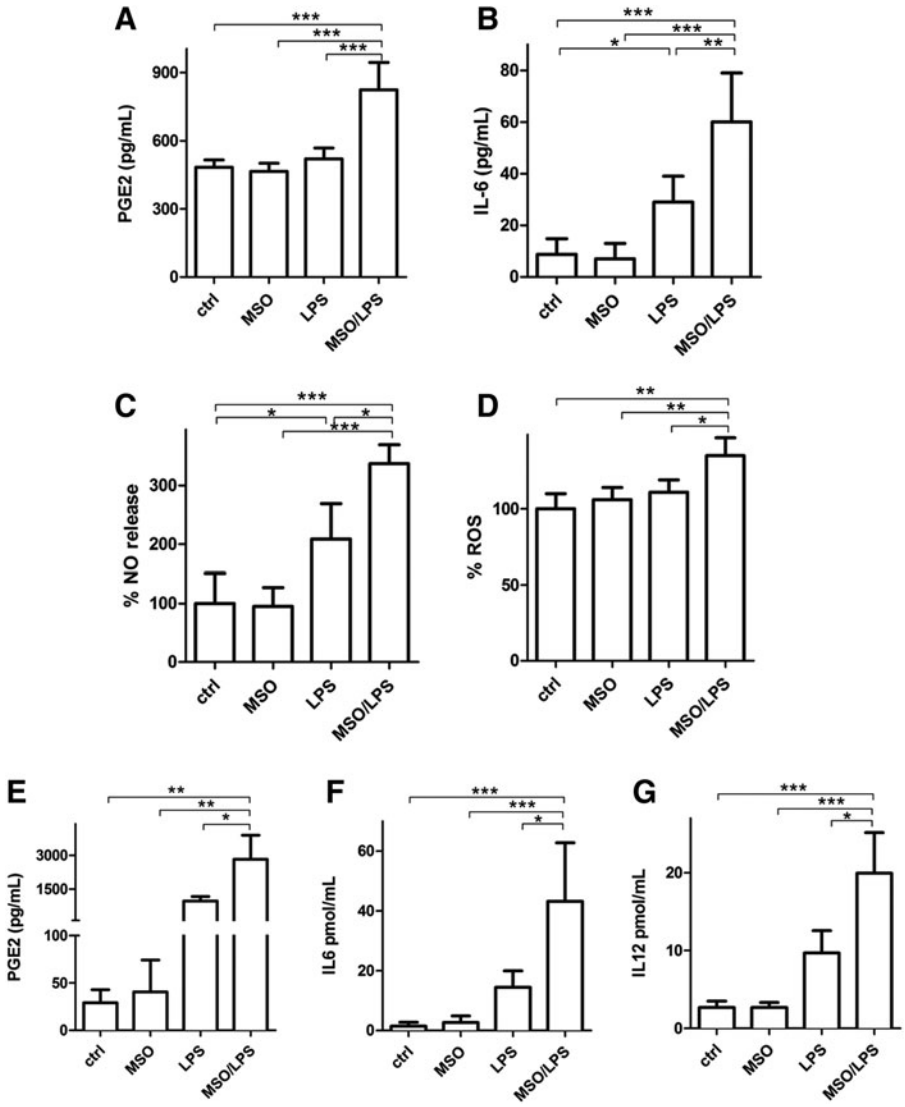

FIG. 2. Release of inflammatory mediators in LPS-activated microglial cells in the presence of GS inhibition. LPS challenge was carried out for 24 h on N9 microglial cells pretreated or not with 1 mM MSO. **(A)** Culture media were assessed for PGE2 by ELISA. Data are reported as mean ± S.D. of four independent experiments. **(B)** Culture media were assessed for IL-6 by ELISA. Data are reported as mean ± S.D. of six independent experiments. **(C, D)** Harvested cells after 24 h were assessed for NO **(C)** and ROS **(D)**, as indicated in the Materials and Methods section. Data are reported as % increase compared with control cells and mean ± S.D. of four independent experiments. Values significantly different between differently treated sample groups are denoted as follows: $*p < 0.05$, $**p < 0.001$, and $***p < 0.0001$. **(E, F)** Culture media from murine primary microglia treated with MSO, LPS, or LPS and MSO were assessed for PGE2 **(E)**, IL-6 **(F)**, and IL-12p40 **(G)** by ELISA. Data are reported as mean ± S.D. of five independent experiments. Values significantly different between differently treated sample groups are denoted as follows: $*p < 0.05$, $**p < 0.001$, and $***p < 0.0001$. NO, nitric oxide; ROS, reactive oxygen species.

GS inhibition impairs insulin-mediated glucose uptake in activated microglia

Based on our data on the role of GS in adipocytes, in which GS inhibition during LPS-induced activation reduces insulin-mediated glucose uptake (unpublished observation), we investigated if also in microglia GS inhibition during LPS activation induces insulin resistance by reducing glucose uptake. Unexpectedly, MSO treatment impaired insulin-mediated glucose uptake in microglia by 72% compared with LPS-treated cells (Fig. 3), suggesting that GS function is much more than a simple metabolic glutamine-synthesizing enzyme as it might recapitulate control of inflammatory response and sensitivity to insulin.

Inhibition of GS in activated microglia mediates neuronal injury

To determine if inhibition of GS in microglia translates into an enhanced ability of these cells to mediate neuronal injury, we focused our attention on murine neuronal N2a cells cultured with LPS and LPS/MSO microglia-conditioned medium.

First of all, we assessed survival of N2a cells exposed to growth media from LPS- and LPS/MSO-treated microglia. Our results demonstrate that microglial-mediated toxicity in neurons exposed to media from LPS/MSO microglia was more pronounced compared with those exposed to media from resting and LPS-treated microglia (Fig. 4A), respectively. Next, we

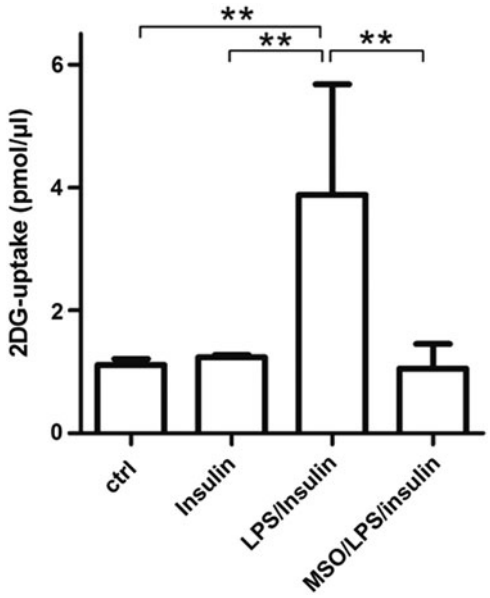

FIG. 3. Insulin-mediated 2-DG uptake in LPS-activated microglia in the presence of GS inhibition. LPS challenge was carried out for 16 h on microglial cells pretreated or not with 1 mM MSO. 2-DG uptake was followed in microglial cells, pretreated or not with 1 μM insulin, by a colorimetric assay kit. The results are presented as mean ± S.D. of four independent experiments. Values significantly higher than those measured in untreated, control microglia cells are denoted as follows: $^{**}p < 0.001$. 2-DG, 2-deoxyglucose.

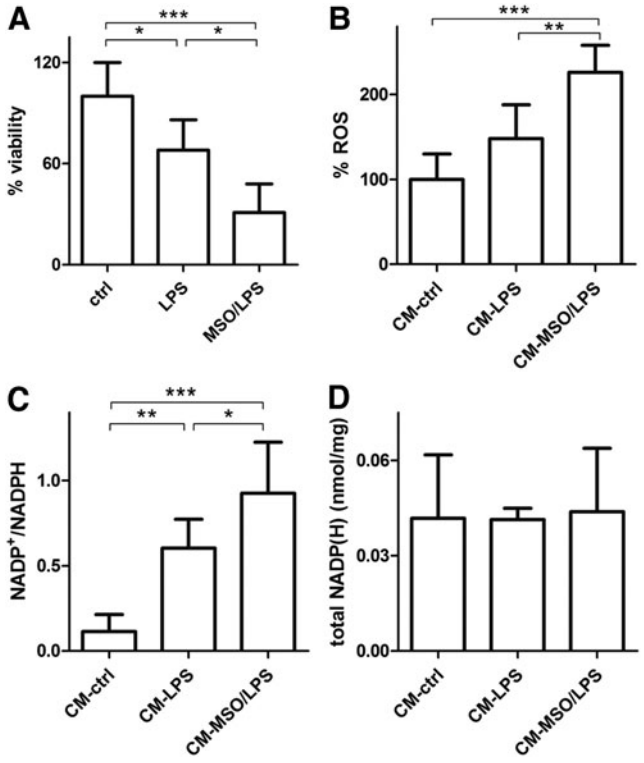

FIG. 4. N2a neuronal cell status upon challenge with CM from LPS-activated microglia. N2a cells were plated and cultured in media collected from 20-h resting (CM), 20-h LPS-activated (CM-LPS), or 20-h LPS-activated, 1 mM MSO (CM-MSO/LPS) pretreated microglial cells. **(A)** Viability was measured with the MTT assay on harvested cells after 18 h. Data are reported as % decrease compared with control cells, mean ± S.D. of five independent experiments. **(B)** N2a cells harvested after 18 h were assessed for ROS, as indicated in the Materials and Methods section. Data are reported as % increase compared with control cells, mean ± S.D. of four independent experiments. **(C, D)** $NADP^+$/NADPH ratios **(C)** and the sums of $NADP^+$+NADPH **(D)** were obtained by LC-MS/MS analysis from harvested cells after 18 h. Values are reported as mean ± S.D. of five independent experiments. Values significantly different between differently treated sample groups are denoted as follows: $^{*}p < 0.05$, $^{**}p < 0.001$, and $^{***}p < 0.0001$. CM, conditioned medium.

verified if this could be associated with changes of the neuronal redox state. We first measured the ROS levels produced by N2a cells exposed to growth media of LPS- and LPS/MSO-treated microglia. N2a cells grown in LPS/MSO-microglial medium displayed higher levels of ROS (+52%) compared with those grown in LPS-treated microglia-derived medium, respectively (Fig. 4B). In line with this finding, N2a intracellular $NADP^+$/NADPH ratios were significantly higher (0.92) compared with those measured in cells grown in LPS-microglial medium (0.58) and also with those from cells grown in resting microglial medium (0.11) (Fig. 4C) with no change of the total $NADP^+$+NADPH pool (Fig. 4D). These data together indicate that the enhanced secretion of proinflammatory and toxic mediators by GS-inhibited activated microglia significantly challenges the neuronal antioxidant endogenous defense, leading eventually to ROS-mediated cell damage and death.

In vivo *microglia-specific genetic ablation of GS strongly enhances inflammatory response to LPSs*

To translate our findings *in vivo*, we obtained a murine model in which GS is specifically knocked out in microglia, which is clearly evident from the GS blot obtained from microglial extracts (Fig. 5). Following gene deletion, we injected LPS to assess the influence of GS on genes upregulated during an inflammatory response. As expected, LPS treatment significantly upregulated the expression of all the tested genes in microglia from both GScKO and control mice. However, in the absence of GS, the induction of M1 markers (except for CXCL9) by LPS was at least twice stronger compared with that measured in microglia from control mice undergoing the same LPS treatment (Fig. 5).

These data clearly confirm that GS plays a role in modulating the response to LPS, and GS gene ablation in microglia exacerbates this inflammatory response.

GS expression is reduced in the spinal cord of the EAE mouse

Having established both *in vitro* and *in vivo* the role of GS in modulating the inflammatory response in activated microglia, we sought to evaluate the relevance of this enzyme in the spinal cords of the EAE mouse, a model of inflammatory autoimmune disease, in which microglia activation is known to play a role. Clinical deficits in these animals are associated with inflammation, as evidenced by the expression of TNF-α, NOS2, and IFNγ in the spinal cords of

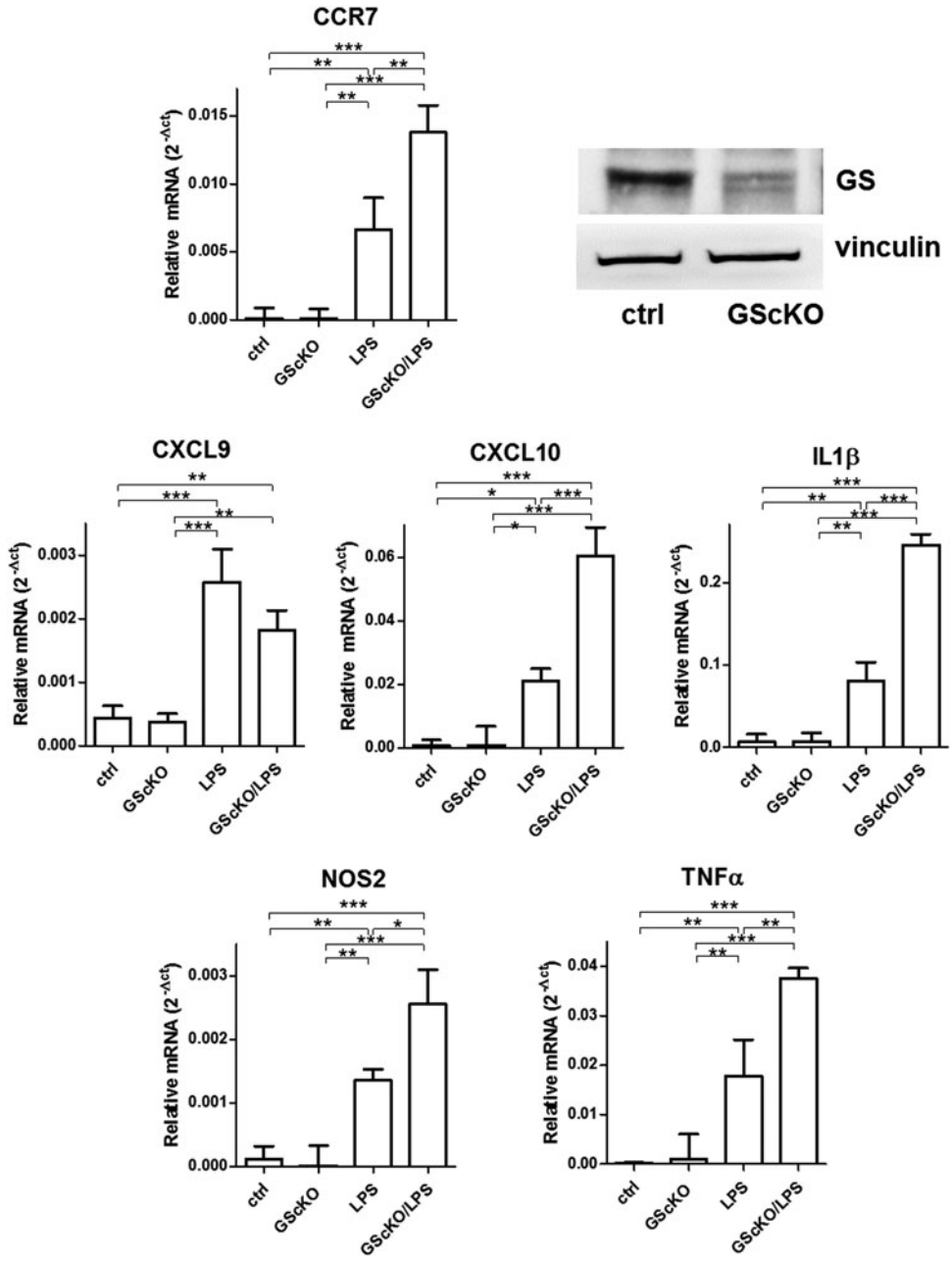

FIG. 5. Expression of inflammatory markers in microglia isolated from LPS-treated control or GScKO mice. qRT-PCR quantification of the inflammatory markers, CCR7, CXCL9, CXCL10, IL-1β, iNOS, and TNF-α, in microglia isolated from LPS-injected control and GScKO mice, in which microglial reduction of GS levels is clearly evident compared with controls (blot *upper right*). Relative mRNA levels in GScKO and control microglia were normalized to the geometric mean of the reference genes, β-actin and glyceraldehyde-3-phosphate dehydrogenase (GAPD). Data are reported as mean ± S.D. of four independent experiments. Values significantly different between differently treated sample groups are denoted as follows: $*p < 0.05$, $**p < 0.001$ and $***p < 0.0001$. GScKO, GS conditional knockout; qRT-PCR, quantitative real-time polymerase chain reaction.

diseased mice (Fig. 6A). Decrease in GS expression was evident already in the spinal cords of mice with clinical scores of 2 and 3, but significantly only in score 5 (57%) (Fig. 6B, C). Glutamine/glutamate levels were also significantly decreased by 66% in score 3 and 75% in score 5 spinal cords (Fig. 6D). Taken together, these data suggest that the loss in GS function might occur with progression of the disease and contribute to the development of inflammatory pathology in the spinal cord of EAE.

Discussion

It is well established that brain microglia express the glutamate scavenging system known to be present in astrocytes, namely the cellular glutamate transporter GLT-1 and GS (12, 44, 69), not only in physiological but also in pathological conditions (11, 28, 65). This expression of GLT-1 and GS by microglia has been explained in two different ways. Microglia may possess a similar mechanism of glutamate scavenging for trophic and protective purposes. Additionally, glutamate uptake from the extracellular spaces might represent a way to enhance GSH production through the coexpression of GLT-1 and the cystine/glutamate antiporter (29, 52, 53).

The present work highlights for the first time the role of glutamate conversion to glutamine in modulating the ability of microglia to respond to the inflammatory stimulus.

In normal conditions, microglia are maintained in a constant state of relative inactivity. At variance with macrophages, basal microglia express low levels of CD45 and major histocompatibility complex class I and II antigens. This can be ascribed to the CNS microenvironment, which is rich in immunomodulatory factors such as TGFβ and is

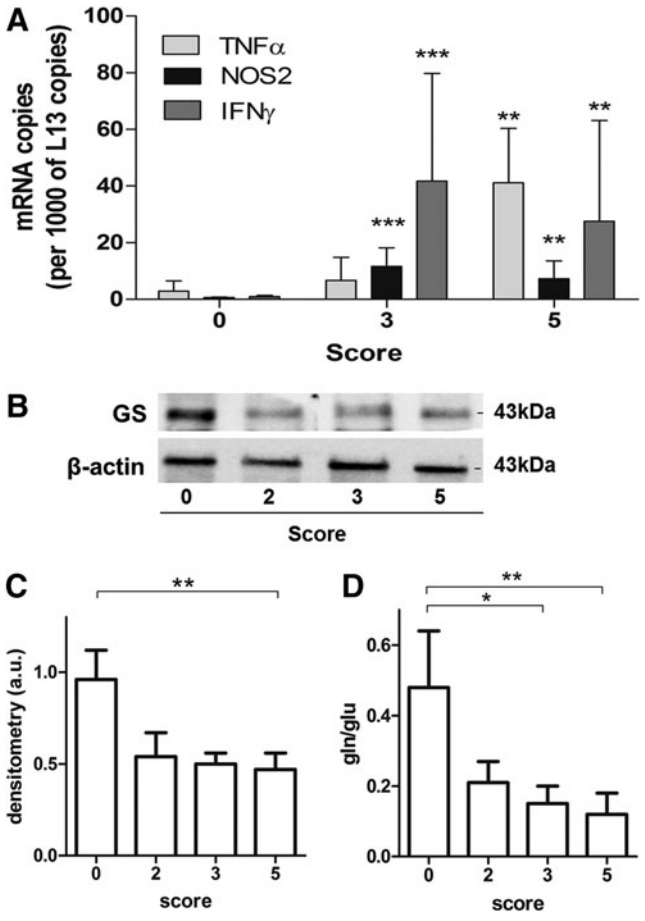

FIG. 6. GS status in EAE spinal cords of MBP-immunized mice at increasing scores of disease severity. **(A)** PLSJL mice were either left nonimmune or immunized with MBP and scored daily for clinical signs of EAE. TNF-α, NOS2, and IFNγ levels were quantified by qRT-PCR in spinal cords from mice with different disease severity levels (0, 3, 5). The results are presented as mean ± S.D. of nine independent experiments and represent the fold increase in the number of copies of specific mRNAs normalized to those of the housekeeping gene L13 mRNA. Expression levels significantly higher than those of similar tissues from score 0 mice are denoted as follows: $^{**}p < 0.01$ and $^{***}p < 0.001$. **(B, C)** GS expression was tested in homogenized spinal cords from mice with different disease severity levels (0, 2, 3, 5). The results are presented as mean ± S.D. of four independent experiments. Values significantly different between different score groups are denoted as follows: $^{**}p < 0.001$. **(D)** Glutamine and glutamate levels were measured by LC-MS/MS analysis from homogenized and extracted spinal cords from mice with different disease severity levels (0, 2, 3, 5). The results are presented as mean ± S.D. of five independent experiments. Glutamine/glutamate ratios significantly different between different score groups are denoted as follows: $^{*}p < 0.05$ and $^{**}p < 0.001$. MBP, myelin basic protein.

protected against potentially stimulatory serum proteins by the blood–brain barrier (BBB) (2). Other resident cells of the CNS are known to modulate microglial phenotype. Principally, not only neurons (66) but also astroglia (40, 55–57) provide inhibitory signals. In this study, we provide evidence of a metabolic mechanism by which microglia control their response to a proinflammatory stimulus. When glutamate conversion to glutamine is inhibited in microglia, their production and release of inflammatory mediators and effectors are elevated, ultimately leading to greater neuronal oxidative stress and injury. Our hypothesis that GS activity might represent an endogenous mechanism controlling the response of microglia to activation, following a given stimulus, is substantiated by the finding that GS activity peaks in the immediate 24 h after LPS treatment before evidence of enhanced expression of GS. Our finding that the increase of GS activity is not perfectly synchronized with GS expression actually confirms previous data, the explanation of which has not been provided (48). It is well known that GS activity is sensitive to oxidative modifications since oxidation-driven loss in protein activity has been associated with many pathological conditions. Due to its particular sensitivity to inactivation by oxidant agents (6, 22, 42, 54), the activity of GS is often used to monitor ROS-mediated brain damage. In a number of conditions, including aging and Alzheimer's disease, as well as in the experimental CNS inflammatory condition, EAE, GS in brain tissues has been found to convert glutamate to glutamine less efficiently than in age-matched normal controls (6, 32, 58), and this event has been linked to its specific oxidation (8). In light of the present findings, it is possible that GS sensitivity to redox balance, which has supported the use of GS as a redox proteomic target in many conditions, represents a physiological mean by which several mechanisms relevant to the inflammatory response are modulated. In this way, GS oxidation might have a functional significance rather than being a marker of ROS-mediated brain damage.

Our data support a beneficial role of GS in controlling the activation of microglia in response to proinflammatory stimuli. GS activity is increased following LPS treatment and its inhibition drives a greater inflammatory response by the cells. This is confirmed *in vitro* both in stimulated N9 and primary microglia, in which pharmacological inhibition of GS during LPS activation significantly increases release of inflammatory mediators. These effects are translated *in vivo*, in which an inducible, microglial-specific GS-deficient mouse expresses to a greater extent inflammatory markers compared with the WT mouse.

Besides sustaining immune response, which is associated with many neurodegenerative disorders (1, 38), the abnormal extracellular environment generated by GS-inhibited activated microglia is destined to strongly impact neuronal function. N2a neuronal cells grown in conditioned media from GS-inhibited microglial cells display decreased viability and increased ROS production at the expense of the intracellular redox balance. Neuronal cell loss might occur through multiple mechanisms. The most conceivable one could be NMDA excitotoxicity and abnormal Ca^{2+} uptake. The excessive Ca^{2+} input to neurons induces neuronal death and, in accordance with our findings in N2a cells, generates excessive ROS that disrupt glutamate transport in neighboring cells (24, 72). With dying neurons, the activation mechanism that maintains microglia in an inflammatory state perpetuates itself, releasing more PGE2, TNF-α, ROS, and so on (62–64, 73). The present evidence on the abnormalities found in the media of GS-inhibited activated microglia points to these mechanisms in different ways. The decreased

glutamine/glutamate ratio due to GS inhibition might interfere with glutamate influx through GLT-1, leading to higher levels of extracellular glutamate, which we measured in the media from LPS-treated microglia upon GS inhibition. In this way, loss of microglial GS activity might impair the described glutamate scavenging system in microglia. Together with glutamate, the NMDA receptor agonist, quinolinic acid, also might perpetuate continuous stimulation on NMDA receptors as its degradation system is rapidly saturated (31, 45, 76). PGE2 might also contribute to neuronal toxicity by increasing Ca^{2+} uptake by neurons (15). TNF-α is also known to activate AMPA and NMDA receptors while decreasing inhibitory $GABA_A$ receptors on neurons (25, 49). Additionally, our finding that GS inhibition reduces insulin-related glucose uptake might shed light into one of the unifying mechanisms controlling insulin resistance, inflammation, and metabolism. Microglial IL-1, IL-6, and TNF-α are known to activate insulin receptor sustrate-1 (IRS-1) serine kinases (IKK, JNK, and Erk2), leading to increased IRS-1 phosphorylation at Ser-307, decreasing its activity (60) as seen in Alzheimer disease (AD) (61). Insulin is known to antagonize the deleterious effects of oxidative stress in the CNS. By stimulating glucose uptake and pyruvate formation, insulin restores intracellular ATP formation, reduces oxidative stress (17), and, more importantly, limits glutamate accumulation in the extrasynaptosomal space, reducing excitotoxicity (18). GS activity might then represent a unifying mechanism being at the interface between inflammation, insulin resistance, and glutamate excitotoxicity.

In the spinal cord of the EAE mouse, GS protein levels decrease together with the glutamine/glutamate ratio. The involvement of microglia in autoimmune pathology is commonly accepted (4, 7, 36) as microglia ablation results in suppression of EAE development and severity (33). Our *in vivo* findings on GScKO mice clearly demonstrate that GS loss represents one of the mechanisms skewing microglia to a more inflammatory phenotype, which might contribute to the progression of autoimmune-mediated damage. Although evaluated in whole tissue, our EAE findings are relevant in the fact that an experimental neurodegenerative condition with a strong inflammatory component, in which microglia play a fundamental role in the progression of the disease, is associated with a loss in the expression of GS. The cause of the loss of GS expression in the EAE spinal cords might be related to oxidative stress, which is known to play a role in several aspects of the pathogenesis of multiple sclerosis (MS) and EAE, including demyelination, axonal injury, and general tissue damage (26, 67), as well as the loss of BBB integrity that allows immune cells to infiltrate CNS tissues (34). ROS production is increased in the CNS inflammatory lesions of EAE and MS (27). Furthermore, GS is known to be oxidized in EAE CNS (9) and in AD brain (8), leading to loss of function (6, 9). In light of the present findings, we propose that inflammatory neurodegeneration is mediated by a sustained inflammatory response with contributions from activated microglia that have lost the anti-inflammatory contribution from GS.

How GS function modulates the cell's ability to respond to a proinflammatory stimulus is of particular interest, but not yet fully resolved for microglia. The fact that GS inhibition interferes with this ability clearly points at cellular glutamine production as a key player. We have recently found that in adipocytes GS activity desensitizes adipocytes to a proinflammatory stimulus by raising intracellular glutamine levels (50), suggesting the role of glutamine as a signaling molecule. This is supported by a strong body of evidence pointing at the intracellular accumulation of glutamine as a mediator regulating many different pathways, such as autophagy, inflammation, mTOR activation, and others (3, 5, 13, 41, 68, 74).

In conclusion, this work unravels a novel mechanism of endogenous modulation of brain inflammation by activated microglia, in which GS activity controls immune response. The consequences of GS inhibition are multiple, ranging from increased release of inflammatory mediators and demise of surrounding cells to modulation of insulin sensitivity. These findings help us to reexamine the significance of GS function and the mechanisms of its activity loss, such as oxidative stress, pointing to a new role of the protein for both the understanding of the pathogenic mechanisms, in which oxidative damage and inflammation occur, and, in perspective, for setting up new strategies of therapeutic intervention.

Materials and Methods

Reagents

Dulbecco's modified Eagle's medium (DMEM), fetal bovine serum (FBS) insulin, bacterial LPSs, MSO, protease inhibitors, phenylmethanesulfonyl fluoride (PMSF), heptafluoro-n-butyric acid (HFBA), and glutamine were obtained from Sigma-Aldrich (St. Louis, MO). Bradford protein assay was obtained from Bio-Rad (Hercules, CA).

Anti-GS primary antibody and the Immobilon Western Chemiluminescent horseradish peroxidase (HRP) substrate were purchased from Millipore (Billerica, MA). Antiactin antivinculin antibodies were purchased from Santa Cruz Biotechnology (Dallas, TX). The HRP-conjugated secondary antibody was obtained from Thermo (Waltham, MA).

Animal models

Experiments with control and GScKO mice were obtained from about 8 weeks old, gender- and age-matched C57Bl/6 littermates raised in a strictly controlled environment. Colony-stimulating factor receptor 1 (CSF1R)-CreERT transgenic mice (CSF1R-CreERT$^{tg/wt}$), provided by J. Pollard (University of Edimbourg, United Kingdom), in which a tamoxifen-induced Cre is under the transcriptional control of human *CSF1R* promoter, were crossed with GS floxed mice ($GS^{L/L}$) obtained from W. Lamers (University of Amsterdam, The Netherlands). The colony was bred by intercrossing $GS^{L/L}$;CSF1R-CreERT$^{tg/wt}$ with $GS^{L/L}$;CSF1R-CreERT$^{wt/wt}$ mice. Mice with macrophage and microglia-specific GS deficiency ($GS^{L/L}$;CSF1R-CreERT$^{tg/wt}$ treated with i.p. injected tamoxifen) are designated as GScKO mice, whereas $GS^{L/L}$;CSF1R-CreERT$^{wt/wt}$ mice (also treated with tamoxifen) are control mice. Construction of targeting vectors and pup genotyping were performed as reported (31a). Acute deletion of GS was obtained by i.p. injection of tamoxifen (1 mg/mouse/day) on both GScKO and control mice for 5 consecutive days. Then, GScKO and control mice received an intraperitoneal injection of LPSs (1 mg/kg) or sterile saline vehicle in a total volume of 100 μl. Twelve hours later, mice were sacrificed and brains were collected for microglia isolation. All procedures were conducted in accordance with federal

guidelines under animal protocols approved by the U.K. Leuven Institutional Animal Care and Use Committee.

As detailed previously (21), female 10- to 11-week-old PLSJL mice (Jackson Laboratories, Bar Harbor, ME) were either left untreated (controls) or immunized s.c. at three sites with 200 μl of an emulsion containing 100 μg of guinea pig myelin basic protein (MBP) in complete Freund's adjuvant supplemented with 4 mg/ml mycobacterium tuberculosis H37RA (BD, Franklin Lakes, NJ). Immunized mice also received 400 ng of pertussis toxin (List Biological Laboratories, Campbell, CA) i.p. on days 0 and 2. The animals were scored daily for clinical signs of EAE. Animals assessed in this study had scores assigned as follows: 0, immunized, but appearing normal; 3, tail paralysis and hindlimb weakness or ataxia; and 5, hindlimb paralysis, but without forelimb involvement, alert, and capable of eating and drinking. Tissue samples were obtained from nonimmunized animals and MBP-immunized mice that had shown clinical signs for at least 3 days with a clinical score of 2, 3, or 5, as well as MBP-immunized mice that did not develop signs of disease (clinical score 0) over the same period of time after immunization. All procedures were conducted in accordance with federal guidelines under animal protocols approved by the Thomas Jefferson University Institutional Animal Care and Use Committee.

Microglial isolation by fluorescence-activated cell sorter sorting

Microglia were isolated from brains of GScKO and WT mice, injected or not with LPSs as previously described (70). In brief, after transcardiac perfusion with ice-cold phosphate-buffered saline (PBS), brains were quickly dissected and mechanically homogenized with a tissue homogenizer in ice-cold Hank's balanced salt solution containing 15 mM HEPES and 0.5% glucose (70). Cells were filtered over a 70-μm strainer and pelleted at 220 g for 10 min at 4°C. Contaminating myelin was removed by resuspending the pellet in 25 ml ice-cold 22% Percoll buffer, overlaying with 5 ml ice-cold PBS, followed by centrifugation in a swinging bucket rotor at 950 *g* for 25 min at 4°C. The cells were incubated with mouse antiCD45-FITC (eBiosciences, Santa Clara, CA) and mouse anti-CD11bAPC (eBiosciences) for 30 min at 4°C in the dark. $CD11b^{high}$/$CD45^{mid}$ cells were isolated using an Aria III fluorescence-activated cell sorter (BD Biosciences, San Jose, CA).

Microglial cells obtained from LPS-injected GScKO and WT mice were collected in RNA lysis buffer provided with the RNeasy microkit (Qiagen) for RT-PCR analysis. Cells from untreated mice were cultured for LPS challenge.

Cell culture

The murine microglial cell line, N9, was cultured in DMEM supplemented with 2 mM glutamine, 10% FBS, 100 U/ml penicillin, and 100 mg/ml streptomycin. Cells were grown at 37°C in a saturated humidified incubator in 95% air and 5% CO2 and were passaged every 3 days. For culturing with various stimulants, N9 cells were distributed into 24-well plates at the density of 1.5×10^5 cells per well in medium, and different stimuli were applied. Cell viability following MSO treatment alone was evaluated with the MTT assay. Cells were stimulated with 100 ng/ml bacterial LPSs from 20 h up to 72 h as described (43). To inhibit GS activity, 1 mM MSO was added to cells right before LPS treatment.

N2a cells (ATCC, Manassas, VA) were grown using the same culture conditions above except for the substitution of 50% Opti-MEM +50% Dulbecco's minimal essential medium in place of the simple DMEM.

Primary microglia isolated from untreated mice were resuspended in DMEM, 10% FBS, 100 U/ml penicillin, 100 μg/ml streptomycin, and N2 supplement and plated at a density of 2.5×10^5 cells per well in a 96-well plate. Once adherent, cells were treated with 100 ng/ml LPSs from 24 h up to 48 h. To inhibit GS activity, 1 mM MSO was added to cells 1 h before LPS treatment.

qRT-PCR analysis

Isolation of mRNA from snap-frozen spinal cords and quantification of specific mRNA levels were performed on tissue samples from nine mice per group by quantitative real-time PCR (qRT-PCR) using previously described primers, probes, and methodologies (9) and a Bio-Rad iCycler iQ real-time detection system (Bio-Rad). Data were calculated based on the threshold cycle (Ct), the PCR cycle at which the fluorescent signal becomes higher than that of the background (cycles 2–10) plus 10 times the SD of the background. Synthetic cDNA standards were used to determine copy numbers. Data are expressed as the fold increase in mRNA copy numbers in test tissues over levels in control tissue samples from naive mice, with all values normalized to the mRNA content of the ribosomal housekeeping protein, L13, in each sample.

RNA isolation and subsequent qRT-PCR analysis from GScKO and WT mice were performed as described (51), with some modifications. The efficiencies of amplification of targeted genes were very near to 100%. Data are expressed as relative mRNA levels (as $2^{-\Delta ct}$) in GScKO and control microglia, with all values normalized to the average mRNA content of two different housekeeping genes (β-actin and glyceraldehyde-3-phosphate dehydrogenase [GAPD]) selected after a survey within a housekeeping gene set.

Western blot analysis

Whole cell lysates were prepared by treating pelleted microglia with ice-cold RIPA buffer (1% Nonidet P-40, 50 mM Tris-HCl pH 7.4, 150 mM NaCl, 0.1% SDS, 2 mM EDTA, 0.5% sodium deoxycholate) containing 1 × protease inhibitors and 1 mM PMSF for 30 min at 4°C.

Homogenates were derived from spinal cord samples and processed as previously described (9, 39). Protein concentration of both lysates was determined by the modified Bradford protein assay and 10 μg of proteins was electrophoresed in a 12% SDS-PAGE under reducing conditions and transferred to nitrocellulose using standard procedures. Anti-GS (Millipore) was used to immunodetect proteins. Western blots were processed also for actin with a specific antibody as an equal total protein loading control. Following incubation with an HRP-conjugated secondary antibody, the immunoreaction was detected by using the Immobilon Western Chemiluminescent HRP Substrate (Millipore).

Metabolite quantification by LC-MS/MS

A total of 2×10^5 cell pellets (0.5 mL cellular medium) were extracted as described (50). Spinal cord tissue was homogenized and extracted as indicated (9). A Quattro Premier

mass spectrometer interfaced with an Acquity UPLC system (Waters, Milford, MA) was used for ESI-LC-MS/MS analysis as described (9). Calibration curves were established using standards and processed under the same conditions as the samples, at five concentrations. The best fit was determined using regression analysis of the peak analyte area. The multiple reaction monitoring transitions in the positive ion mode were *m/z* 148.2 > 83.9 for glutamate, *m/z* 147.2 > 83.9 for glutamine, *m/z* 744.1 > 507.8 for $NADP^+$, and *m/z* 746.0 > 729.0 for NADPH, and the chromatographic resolution was obtained as indicated. Chromatographic resolution was achieved as indicated (9, 35, 50, 51, 75) with a flow rate set at 0.3 ml/min. Quinolinic acid was monitored at *m/z* 168.0 > 78.2 and the chromatographic resolution was obtained with an HT3 column (Waters).

GS activity assay

GS activity was followed as indicated (9). Briefly, 900 μl of reaction cocktail (final concentration in the reaction mix: 34.1 mM imidazole, 102 mM glutamate, 8.5 mM ATP, 60 mM $MgCl_2$, 18.9 mM KCl, 45 mM NH_4Cl, pH 7.1) was placed into a quartz cuvette. Phosphoenolpyruvate (final concentration 1.1 mM), freshly prepared NADH (final concentration 0.25 mM), pyruvate kinase (EC 2.7.1.40, 28 U), lactate dehydrogenase (EC 1.1.1.27, 40 U), and 200 μg of cell proteins were added to a 1 ml final volume. NADH levels were followed for 10 min in a Varian Cary 50 spectrophotometer (Agilent Technologies, Santa Clara, CA) (A 340 nm, T 37°C).

Enzyme-linked immunosorbent assays for PGE2 and IL-6 and IL-12

To measure cytokines, either 1.5×10^5 N9 or 2.5×10^5 primary microglial cells were treated with LPSs and LPS plus 1 mM MSO, as indicated above. After 48 h, 100 μl of the cellular media supernatants from N9 cells were assayed for PGE2 with a DetectX High Sensitivity PGE2 Enzyme Immunoassay Kit (Arbor Assays, Ann Arbor, MI), as indicated (50). For IL-6 and IL-12p40 detection, medium supernatants from primary microglia were tested with mouse enzyme-linked immunosorbent assay (ELISA) kits from eBioscience (San Diego, CA). Experimentation was performed following the manufacturer's protocol.

NO and ROS detection

Nitrite, the oxidation product of NO, was measured using the Griess reaction (30). For ROS analysis, the cells were incubated with 10 μM DCFH-DA (2′,7′-dichloro-dihydrofluorescein diacetate; Molecular Probes, Eugene, OR) for 30 min. The fluorescence was measured by a Victor3 plate reader (PerkinElmer, Whaltam, MA) at 485 nm excitation and 530 nm emission wavelengths (71).

Glucose uptake assay

Glucose uptake assay was determined as previously described with modifications. After treatments, N9 microglia cells were starved in low-glucose DMEM with 0.5% serum for 16 h (46); cells were washed twice with 37°C Krebs-Ringer phosphate (KRP) buffer (pH 7.4) (128 mM NaCl, 4.7 mM KCl, 1.65 mM $CaCl_2$, 2.5 mM $MgSO_4$, and 5 mM Na_2HPO_4). Cells were either left untreated or treated with insulin (1 μM) for 20 min in KRP buffer. Glucose uptake was started by addition of 1 mM 2-deoxy-D-glucose (2-DG) for an additional 20 min at 37°C. Cells were gently washed three times with ice-cold DPBS and lysed. Sample was assayed using the Colorimetric Glucose Uptake Assay kit from Abcam (Cambridge, United Kingdom).

Conditioned medium and neuronal viability assay

N9 cells were seeded into 24-well plates and then switched to a serum-free medium. Cells were then exposed to 100 ng/ml of LPSs for 4 h with or without 1 mM MSO, after which cells were rinsed to remove LPSs, and then allowed to incubate for an additional 24 h in fresh serum-free medium. This conditioned medium was then collected and applied immediately to N2a cells for 18 h, after which N2a cell viability was determined using MTT (16). Neuronal cells and the conditioned media were processed for mass spectrometry analysis.

Cell viability

Cell viability was evaluated by 3-(4,5-dimethylthiazol-2-yl)-2,5-diphenyltetrazolium bromide (MTT) assay; 1×10^4 cells were seeded in a 96-well plate, then 25 μl of MTT solution (2.5 mg/ml) was added to each well and incubated for 4 h. Media were removed and 200 μl DMSO was added to each well and incubated for 30 min at room temperature with shaking to dissolve the Formazan crystal completely. The optical density was measured in a 96-well plate reader (PerkinElmer) at 570 nm.

Statistical analyses

Data entry and all analyses were performed in a blinded manner. Results are shown as mean ± S.D. Statistical significance was calculated by ANOVA test with Tukey's *post hoc* test, whereas EAE data were analyzed with Kruskal–Wallis test with Dunn's multiple comparison test. Data were considered statistically significant as follows: $*p < 0.05$, $**p < 0.001$, and $***p < 0.0001$.

Acknowledgments

The authors are very grateful to W.H. Lamers for providing the $GS^{L/L}$ mouse and J. Pollard for providing the CSF1R-$CreERT^{tg/wt}$ mouse. E.M.P. was short-term EMBO fellow. This research received funding from the Italian Ministry of Education, University and Research (MIUR), the University of Bari ''Aldo Moro'', and from the European Research Council.

Author Disclosure Statement

No competing financial interests exist.

References

1. Abcouwer SF, Shanmugam S, Gomez PF, Shushanov S, Barber AJ, Lanoue KF, Quinn PG, Kester M, and Gardner TW. Effect of IL-1β on survival and energy metabolism of R28 and RGC-5 retinal neurons. *Investig Opthalmology Vis Sci* 49: 5581–5592, 2008.
2. Adams RA, Bauer J, Flick MJ, Sikorski SL, Nuriel T, Lassmann H, Degen JL, and Akassoglou K. The fibrin-derived gamma377-395 peptide inhibits microglia activation and suppresses relapsing paralysis in central nervous system autoimmune disease. *J Exp Med* 204: 571–582, 2007.

3. Ban K, Sprunt JM, Martin S, Yang P, and Kozar RA. Glutamine activates peroxisome proliferator-activated receptor-γ in intestinal epithelial cells via 15-S-HETE and 13-OXO-ODE: a novel mechanism. *Am J Physiol Gastrointest Liver Physiol* 301: G547–G554, 2011.
4. Benveniste EN. Role of macrophages/microglia in multiple sclerosis and experimental allergic encephalomyelitis. *J Mol Med (Berl)* 75: 165–173, 1997.
5. Brasse-Lagnel C, Lavoinne A, Loeber D, Fairand A, Bôle-Feysot C, Deniel N, and Husson A. Glutamine and interleukin-1beta interact at the level of Sp1 and nuclear factor-kappaB to regulate argininosuccinate synthetase gene expression. *FEBS J* 274: 5250–5262, 2007.
6. Butterfield DA, Hensley K, Cole P, Subramaniam R, Aksenov M, Aksenova M, Bummer PM, Haley BE, and Carney JM. Oxidatively induced structural alteration of glutamine synthetase assessed by analysis of spin label incorporation kinetics: relevance to Alzheimer's disease. *J Neurochem* 68: 2451–2457, 1997.
7. Carson MJ. Microglia as liaisons between the immune and central nervous systems: functional implications for multiple sclerosis. *Glia* 40: 218–231, 2002.
8. Castegna A, Aksenov M, Aksenova M, Thongboonkerd V, Klein JB, Pierce WM, Booze R, Markesbery WR, and Butterfield DA. Proteomic identification of oxidatively modified proteins in Alzheimer's disease brain. Part 1: creatine kinase bb, glutamine synthase, and ubiquitin carboxy-terminal hydrolase L-1. *Free Radic Biol Med* 33: 562–571, 2002.
9. Castegna A, Palmieri L, Spera I, Porcelli V, Palmieri F, Fabis-Pedrini MJ, Kean RB, Barkhouse DA, Curtis MT, and Hooper DC. Oxidative stress and reduced glutamine synthetase activity in the absence of inflammation in the cortex of mice with experimental allergic encephalomyelitis. *Neuroscience* 185: 97–105, 2011.
10. Cherry JD, Olschowka JA, and O'Banion MK. Neuroinflammation and M2 microglia: the good, the bad, and the inflamed. *J Neuroinflammation* 11: 98, 2014.
11. Chrétien F, Le Pavec G, Vallat-Decouvelaere A-V, Delisle M-B, Uro-Coste E, Ironside JW, Gambetti P, Parchi P, Créminon C, Dormont D, Mikol J, Gray F, and Gras G. Expression of excitatory amino acid transporter-1 (EAAT-1) in brain macrophages and microglia of patients with prion diseases. *J Neuropathol Exp Neurol* 63: 1058–1071, 2004.
12. Chrétien F, Vallat-Decouvelaere AV, Bossuet C, Rimaniol AC, Le Grand R, Le Pavec G, Créminon C, Dormont D, Gray F, and Gras G. Expression of excitatory amino acid transporter-2 (EAAT-2) and glutamine synthetase (GS) in brain macrophages and microglia of SIVmac251-infected macaques. *Neuropathol Appl Neurobiol* 28: 410–417, 2002.
13. Cohen A and Hall MN. An amino acid shuffle activates mTORC1. *Cell* 136: 399–400, 2009.
14. Cooper AJ and Plum F. Biochemistry and physiology of brain ammonia. *Physiol Rev* 67: 440–519, 1987.
15. Davidson JM, Wong CT, Rai-Bhogal R, Li H, and Crawford DA. Prostaglandin E2 elevates calcium in differentiated neuroectodermal stem cells. *Mol Cell Neurosci* 74: 71–77, 2016.
16. Dimayuga FO, Wang C, Clark JM, Dimayuga ER, Dimayuga VM, and Bruce-Keller AJ. SOD1 overexpression alters ROS production and reduces neurotoxic inflammatory signaling in microglial cells. *J Neuroimmunol* 182: 89–99, 2007.
17. Duarte AI, Proença T, Oliveira CR, Santos MS and Rego AC. Insulin restores metabolic function in cultured cortical neurons subjected to oxidative stress. *Diabetes* 55: 2863–2870, 2006.
18. Duarte AI, Santos MS, Seiça R, and de Oliveira CR. Insulin affects synaptosomal GABA and glutamate transport under oxidative stress conditions. *Brain Res* 977: 23–30, 2003.
19. Eid T, Tu N, Lee T-SW, and Lai JCK. Regulation of astrocyte glutamine synthetase in epilepsy. *Neurochem Int* 63: 670–681, 2013.
20. Eisenberg D, Gill HS, Pfluegl GM, and Rotstein SH. Structure-function relationships of glutamine synthetases. *Biochim Biophys Acta* 1477: 122–145, 2000.
21. Fabis MJ, Scott GS, Kean RB, Koprowski H, and Hooper DC. Loss of blood-brain barrier integrity in the spinal cord is common to experimental allergic encephalomyelitis in knockout mouse models. *Proc Natl Acad Sci U S A* 104: 5656–5661, 2007
22. Fisher MT and Stadtman ER. Oxidative modification of *Escherichia coli* glutamine synthetase. Decreases in the thermodynamic stability of protein structure and specific changes in the active site conformation. *J Biol Chem* 267: 1872–1880, 1992.
23. Frank-Cannon TC, Alto LT, McAlpine FE, and Tansey MG. Does neuroinflammation fan the flame in neurodegenerative diseases? *Mol Neurodegener* 4: 47, 2009.
24. Gao X, Kim HK, Mo Chung J, and Chung K. Reactive oxygen species (ROS) are involved in enhancement of NMDA-receptor phosphorylation in animal models of pain. *Pain* 131: 262–271, 2007.
25. Gelbard HA, Dzenko KA, DiLoreto D, del Cerro C, del Cerro M, and Epstein LG. Neurotoxic effects of tumor necrosis factor alpha in primary human neuronal cultures are mediated by activation of the glutamate AMPA receptor subtype: implications for AIDS neuropathogenesis. *Dev Neurosci* 15: 417–422, 1993.
26. Gilgun-Sherki Y, Melamed E, and Offen D. The role of oxidative stress in the pathogenesis of multiple sclerosis: the need for effective antioxidant therapy. *J Neurol* 251: 261–268, 2004.
27. Gonsette RE. Neurodegeneration in multiple sclerosis: the role of oxidative stress and excitotoxicity. *J Neurol Sci* 274: 48–53, 2008.
28. Gras G, Chrétien F, Vallat-Decouvelaere A-V, Le Pavec G, Porcheray F, Bossuet C, Léone C, Mialocq P, Dereuddre-Bosquet N, Clayette P, Le Grand R, Créminon C, Dormont D, Rimaniol A-C, and Gray F. Regulated expression of sodium-dependent glutamate transporters and synthetase: a neuroprotective role for activated microglia and macrophages in HIV infection?. *Brain Pathol* 13: 211–222, 2003.
29. Gras G, Porcheray F, Samah B, and Leone C. The glutamate-glutamine cycle as an inducible, protective face of macrophage activation. *J Leukoc Biol* 80: 1067–1075, 2006.
30. Green LC, Wagner DA, Glogowski J, Skipper PL, Wishnok JS, and Tannenbaum SR. Analysis of nitrate, nitrite, and [15N]nitrate in biological fluids. *Anal Biochem* 126: 131–138, 1982.
31. Guillemin GJ. Quinolinic acid, the inescapable neurotoxin. *FEBS J* 279: 1356–1365, 2012.
31a. He Y, Hakvoort TB, Vermeulen JL, Labruyère WT, De Waart DR, Van Der Hel WS, Ruijter JM, Uylings HB, and Lamers WH. Glutamine synthetase deficiency in murine astrocytes results in neonatal death. *Glia* 58: 741–754, 2010.
32. Hensley K, Hall N, Subramaniam R, Cole P, Harris M, Aksenov M, Aksenova M, Gabbita SP, Wu JF, Carney JM, Lovell M, Markesbery WR, and Butterfield DA. Brain regional correspondence between Alzheimer's disease histopathology and biomarkers of protein oxidation. *J Neurochem* 65: 2146–2156, 2002.

33. Heppner FL, Greter M, Marino D, Falsig J, Raivich G, Hövelmeyer N, Waisman A, Rülicke T, Prinz M, Priller J, Becher B, and Aguzzi A. Experimental autoimmune encephalomyelitis repressed by microglial paralysis. *Nat Med* 11: 146–152, 2005.
34. Hooper DC, Ohnishi ST, Kean R, Numagami Y, Dietzschold B, and Koprowski H. Local nitric oxide production in viral and autoimmune diseases of the central nervous system. *Proc Natl Acad Sci U S A* 92: 5312–5316, 1995.
35. Infantino V, Castegna A, Iacobazzi F, Spera I, Scala I, Andria G, and Iacobazzi V. Impairment of methyl cycle affects mitochondrial methyl availability and glutathione level in Down's syndrome. *Mol Genet Metab* 102: 378–382, 2011.
36. Jack C, Ruffini F, Bar-Or A, and Antel JP. Microglia and multiple sclerosis. *J Neurosci Res* 81: 363–373, 2005.
37. Jenstad M, Quazi AZ, Zilberter M, Haglerod C, Berghuis P, Saddique N, Goiny M, Buntup D, Davanger S, S Haug FM, Barnes CA, McNaughton BL, Ottersen OP, Storm-Mathisen J, Harkany T, and Chaudhry FA. System A transporter SAT2 mediates replenishment of dendritic glutamate pools controlling retrograde signaling by glutamate. *Cereb Cortex* 19: 1092–1106, 2009.
38. Koprich JB, Reske-Nielsen C, Mithal P, and Isacson O. Neuroinflammation mediated by IL-1beta increases susceptibility of dopamine neurons to degeneration in an animal model of Parkinson's disease. *J Neuroinflammation* 5: 8, 2008.
39. Kung HN, Marks JR, and Chi JT. Glutamine synthetase is a genetic determinant of cell type-specific glutamine independence in breast epithelia. *PLoS Genet* 7: e100229, 2011.
40. Leone C, Le Pavec G, Même W, Porcheray F, Samah B, Dormont D, and Gras G. Characterization of human monocyte-derived microglia-like cells. *Glia* 54: 183–192, 2006.
41. Lesueur C, Bôle-Feysot C, Bekri S, Husson A, Lavoinne A, and Brasse-Lagnel C. Glutamine induces nuclear degradation of the NF-κB p65 subunit in Caco-2/TC7 cells. *Biochimie* 94: 806–815, 2012.
42. Levine RL. Oxidative modification of glutamine synthetase. II. Characterization of the ascorbate model system. *J Biol Chem* 258: 11828–11833, 1983.
43. Liu HC, Zheng MH, Du YL, Wang L, Kuang F, Qin HY, Zhang BF, and Han H. N9 microglial cells polarized by LPS and IL4 show differential responses to secondary environmental stimuli. *Cell Immunol* 278: 84–90, 2012.
44. López-Redondo F, Nakajima K, Honda S, and Kohsaka S. Glutamate transporter GLT-1 is highly expressed in activated microglia following facial nerve axotomy. *Brain Res Mol Brain Res* 76: 429–435, 2000.
45. Lugo-Huitrón R, Ugalde Muñiz P, Pineda B, Pedraza-Chaverrí J, Ríos C, and Pérez-de la Cruz V. Quinolinic acid: an endogenous neurotoxin with multiple targets. *Oxid Med Cell Longev* 2013: 104024, 2013.
46. Lumeng CN, Bodzin JL, and Saltiel AR. Obesity induces a phenotypic switch in adipose tissue macrophage polarization. *J Clin Invest* 117: 175–184, 2007.
47. Martinez-Hernandez A, Bell KP, and Norenberg MD. Glutamine synthetase: glial localization in brain. *Science* 195: 1356–1358, 1977.
48. Nakajima K, Kanamatsu T, Takezawa Y, and Kohsaka S. Up-regulation of glutamine synthesis in microglia activated with endotoxin. *Neurosci Lett* 591: 99–104, 2015.
49. Olmos G and Lladó J. Tumor necrosis factor alpha: a link between neuroinflammation and excitotoxicity. *Mediators Inflamm* 2014: 861231, 2014.
50. Palmieri EM, Spera I, Menga A, Infantino V, Iacobazzi V, and Castegna A. Glutamine synthetase desensitizes differentiated adipocytes to proinflammatory stimuli by raising intracellular glutamine levels. *FEBS Lett* 588: 4807–4814, 2014.
51. Palmieri EM, Spera I, Menga A, Infantino V, Porcelli V, Iacobazzi V, Pierri CL, Hooper DC, Palmieri F, and Castegna A. Acetylation of human mitochondrial citrate carrier modulates mitochondrial citrate/malate exchange activity to sustain NADPH production during macrophage activation. *Biochim Biophys Acta* 1847: 729–738, 2015.
52. Persson M, Sandberg M, Hansson E, and Rönnbäck L. Microglial glutamate uptake is coupled to glutathione synthesis and glutamate release. *Eur J Neurosci* 24: 1063–1070, 2006.
53. Rimaniol AC, Mialocq P, Clayette P, Dormont D, and Gras G. Role of glutamate transporters in the regulation of glutathione levels in human macrophages. *Am J Physiol Cell Physiol* 281: C1964–C1970, 2001.
54. Rivett AJ and Levine RL. Metal-catalyzed oxidation of *Escherichia coli* glutamine synthetase: correlation of structural and functional changes. *Arch Biochem Biophys* 278: 26–34, 1990.
55. Rosenstiel P, Lucius R, Deuschl G, Sievers J, and Wilms H. From theory to therapy: implications from an in vitro model of ramified microglia. *Microsc Res Tech* 54: 18–25, 2001.
56. Schmidtmayer J, Jacobsen C, Miksch Gm, and Sievers J. Blood monocytes and spleen macrophages differentiate into microglia-like cells on monolayers of astrocytes: membrane currents. *Glia* 12: 259–267, 1994.
57. Sievers J, Parwaresch R, and Wottge HU. Blood monocytes and spleen macrophages differentiate into microglia-like cells on monolayers of astrocytes: morphology. *Glia* 12: 245–258, 1994.
58. Smith CD, Carney JM, Starke-Reed PE, Oliver CN, Stadtman ER, Floyd RA, and Markesbery WR. Excess brain protein oxidation and enzyme dysfunction in normal aging and in Alzheimer disease. *Proc Natl Acad Sci U S A* 88: 10540–10543, 1991.
59. Smith JA, Das A, Ray SK, and Banik NL. Role of pro-inflammatory cytokines released from microglia in neurodegenerative diseases. *Brain Res Bull* 87: 10–20, 2012.
60. Steen E, Terry BM, Rivera EJ, Cannon JL, Neely TR, Tavares R, Xu XJ, Wands JR, and de la Monte SM. Impaired insulin and insulin-like growth factor expression and signaling mechanisms in Alzheimer's disease—is this type 3 diabetes? *J Alzheimers Dis* 7: 63–80, 2005.
61. Talbot K, Wang H-Y, Kazi H, Han L-Y, Bakshi KP, Stucky A, Fuino RL, Kawaguchi KR, Samoyedny AJ, Wilson RS, Arvanitakis Z, Schneider JA, Wolf BA, Bennett DA, Trojanowski JQ, and Arnold SE. Demonstrated brain insulin resistance in Alzheimer's disease patients is associated with IGF-1 resistance, IRS-1 dysregulation, and cognitive decline. *J Clin Invest* 122: 1316–1338, 2012.
62. Tamiji J and Crawford DA. Prostaglandin E2 and misoprostol induce neurite retraction in Neuro-2a cells. *Biochem Biophys Res Commun* 398: 450–456, 2010.
63. Tamiji J and Crawford DA. Misoprostol elevates intracellular calcium in Neuro-2a cells via protein kinase A. *Biochem Biophys Res Commun* 399: 565–570, 2010.
64. Uttara B, Singh AV, Zamboni P, and Mahajan RT. Oxidative stress and neurodegenerative diseases: a review of upstream and downstream antioxidant therapeutic options. *Curr Neuropharmacol* 7: 65–74, 2009.
65. Vallat-Decouvelaere AV, Chrétien F, Gras G, Le Pavec G, Dormont D, and Gray F. Expression of excitatory amino acid transporter-1 in brain macrophages and microglia of

HIV-infected patients. A neuroprotective role for activated microglia?. *J Neuropathol Exp Neurol* 62: 475–485, 2003.
66. Van Beek EM, Cochrane F, Barclay AN, and van den Berg TK. Signal regulatory proteins in the immune system. *J Immunol* 175: 7781–7787, 2005.
67. Van der Goes A, Brouwer J, Hoekstra K, Roos D, van den Berg TK, and Dijkstra CD. Reactive oxygen species are required for the phagocytosis of myelin by macrophages. *J Neuroimmunol* 92: 67–75, 1998.
68. Van der Vos KE, Eliasson P, Proikas-Cezanne T, Vervoort SJ, van Boxtel R, Putker M, van Zutphen IJ, Mauthe M, Zellmer S, Pals C, Verhagen LP, Groot Koerkamp MJ, Braat AK, Dansen TB, Holstege FC, Gebhardt R, Burgering BM, and Coffer PJ. Modulation of glutamine metabolism by the PI(3)K-PKB-FOXO network regulates autophagy. *Nat Cell Biol* 14: 829–837, 2012.
69. Van Landeghem FK, Stover JF, Bechmann I, Brück W, Unterberg A, Bührer C, and von Deimling A. Early expression of glutamate transporter proteins in ramified microglia after controlled cortical impact injury in the rat. *Glia* 35: 167–179, 2001.
70. Verheijden S, Beckers L, Casazza A, Butovsky O, Mazzone M, and Baes M. Identification of a chronic non-neurodegenerative microglia activation state in a mouse model of peroxisomal β-oxidation deficiency. *Glia* 63: 1606–1620, 2015.
71. Wang H and Joseph JA. Quantifying cellular oxidative stress by dichlorofluorescein assay using microplate reader. *Free Radic Biol Med* 27: 612–616, 1999.
72. Wang JY, Chi SI, Wang JY, Hwang CP, and Wang JY. Effects of various nitric oxide synthase inhibitors on NMDA-induced neuronal injury in rat cortical neurons. *Chin J Physiol* 39: 227–233, 1996
73. Wong CT, Ahmad E, Li H, and Crawford DA. Prostaglandin E2 alters Wnt-dependent migration and proliferation in neuroectodermal stem cells: implications for autism spectrum disorders. *Cell Commun Signal* 12: 19, 2014.
74. Xue H, Slavov D, and Wischmeyer PE. Glutamine-mediated dual regulation of heat shock transcription factor-1 activation and expression. *J Biol Chem* 287: 40400–40413, 2012.
75. Zallot R, Agrimi G, Lerma-Ortiz C, Teresinski HJ, Frelin O, Ellens KW, Castegna A, Russo A, de Crécy-Lagard V, Mullen RT, Palmieri F, and Hanson AD. Identification of mitochondrial coenzyme a transporters from maize and Arabidopsis. *Plant Physiol* 162: 581–588, 2013.
76. Zinger A, Barcia C, Herrero MT, and Guillemin GJ. The involvement of neuroinflammation and kynurenine pathway in Parkinson's disease. *Parkinsons Dis* 2011: 716859, 2011.

Address correspondence to:
Prof. Massimiliano Mazzone
Laboratory of Tumor Inflammation and Angiogenesis
Department of Oncology
VIB Vesalius Research Center
University of Leuven
Herestraat 49, box 912
Leuven B-3000
Belgium

E-mail: massimiliano.mazzone@vib-kuleuven.be

Prof. Alessandra Castegna
Department of Biosciences, Biotechnology and Biopharmaceutics
University of Bari
Via Orabona 7
Bari 70125
Italy

E-mail: alessandra.castegna@uniba.it

Date of first submission to ARS Central, March 31, 2016; date of final revised submission, September 23, 2016; date of acceptance, September 29, 2016.

Abbreviations Used

BBB = blood–brain barrier
CM = conditioned medium
CSF1R = colony-stimulating factor 1 receptor
Ctrl mice = $GS^{L/L}$;CSFR1-$Cre^{wt/wt}$ tamoxifen-injected mice
DCFH-DA = dichloro-dihydro-fluorescein diacetate
2-DG = 2-deoxy-glucose
DMEM = Dulbecco's modified Eagle's medium
EAE = experimental autoimmune encephalomyelitis
EDTA = ethylenediaminetetraacetic acid
FBS = fetal bovine serum
GADP = glyceraladehyde-3-phosphate dehydrogenase
GLT-1 = glutamate type I transporter
GS = glutamine synthetase
GS cKO mice = $GS^{L/L}$;CSFR1-$Cre^{tg/wt}$ tamoxifen-injected mice
GSH = reduced glutathione
HRP = horseradish peroxidase
IL-6 = interleukin-6
IL-12 = interleukin-12
IRS-1 = insulin receptor sustrate-1
LC-ESI-MS/MS = liquid chromatography–electrospray ionization tandem mass spectrometry
LPS = lipopolysaccharide
MBP = myelin basic protein
MS = multiple sclerosis
MSO = methionine sulfoximine
MTT = 3-(4,5-dimethylthiazol-2-yl)-2,5-diphenyltetrazolium bromide
NADP(H) = nicotinamide adenine dinucleotide phosphate (reduced)
NMDA = N-methyl-D-aspartate
NO = nitric oxide
PMSF = phenylmethylsulfonyl fluoride
PGE2 = prostaglandin E2
qRT-PCR = quantitative real-time polymerase chain reaction
ROS = reactive oxygen species
TGFβ = transforming growth factor beta